

Mapping of C^* Elements in Finite Element Method using Transformation Matrix

G. H. Majzoob, and B. Sharifi Hamadani

Abstract—Mapping between local and global coordinates is an important issue in finite element method, as all calculations are performed in local coordinates. The concern arises when sub-parametric are used, in which the shape functions of the field variable and the geometry of the element are not the same. This is particularly the case for C^* elements in which the extra degrees of freedoms added to the nodes make the elements sub-parametric. In the present work, transformation matrix for C^{1*} (an 8-noded hexahedron element with 12 degrees of freedom at each node) is obtained using equivalent C^0 elements (with the same number of degrees of freedom). The convergence rate of 8-noded C^{1*} element is nearly equal to its equivalent C^0 element, while it consumes less CPU time with respect to the C^0 element. The existence of derivative degrees of freedom at the nodes of C^{1*} element along with excellent convergence makes it superior compared with its equivalent C^0 element.

Keywords—Mapping, Finite element method, C^* elements, Convergence, C^0 elements.

I. MAPPING CONCEPT

ELEMENTS are divided into 3 categories in finite element method. These are: iso-parametric, sub-parametric and super-parametric elements. Iso-parametric elements are those in which the shape functions for both the field variable and the geometry of the element are the same. For two dimensional iso-parametric elements we have:

$$x = \sum_{i=1}^n N_i x_i, \quad y = \sum_{i=1}^n N_i y_i, \quad \varphi = \sum_{i=1}^n N_i \varphi_i \quad (1)$$

All calculations in finite element methods are usually carried out in local coordinates, ξ and η . The transformation between derivatives of shape functions in global and local coordinates for two dimensional iso-parametric elements is performed using Jacobian matrix which is defined as follow:

$$\begin{bmatrix} \frac{\partial N_i}{\partial \xi} \\ \frac{\partial N_i}{\partial \eta} \end{bmatrix} = \begin{bmatrix} \sum_{i=1}^n N_i x_i / \partial \xi & \sum_{i=1}^n N_i y_i / \partial \xi \\ \sum_{i=1}^n N_i x_i / \partial \eta & \sum_{i=1}^n N_i y_i / \partial \eta \end{bmatrix} \begin{bmatrix} \frac{\partial N_i}{\partial x} \\ \frac{\partial N_i}{\partial y} \end{bmatrix} = [J] \begin{bmatrix} \frac{\partial N_i}{\partial x} \\ \frac{\partial N_i}{\partial y} \end{bmatrix} \quad (2)$$

Manuscript received 15 December, 2006. This work is part of a MSc thesis conducted at Azad university, Hamadan, Iran.

G. H. Majzoobi is a member of academic staff of Azad university in Takestan, Iran. Tel: 0098-282-5226945, Fax: 0098-282-5226016, e-mail: gh_majzoobi@yahoo.co.uk..

B. Sharifi Hamadani is a member of academic staff of Hamadan Azad University in Hamadan, Iran.

Equation (1) for super-parametric and sub-parametric elements is defined as follows [2]:

$$x = \sum_{i=1}^n N'_i x_i, \quad y = \sum_{i=1}^n N'_i y_i, \quad (3)$$

$$\varphi = \sum_{i=1}^m N_i \varphi_i, \quad N'_i \neq N_i \quad (m \neq n)$$

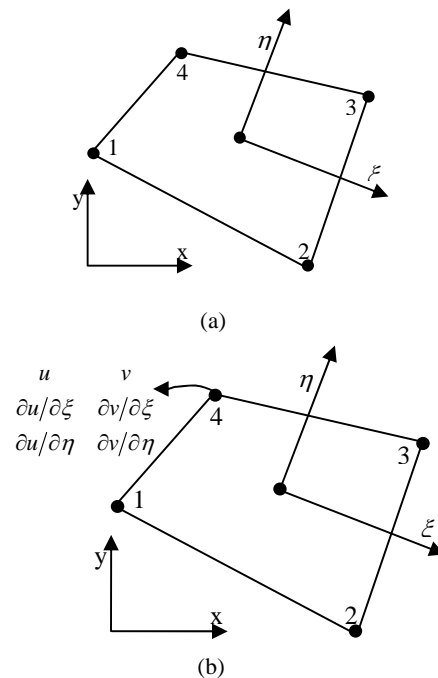


Fig. 1 (a) An element with global and local coordinates and (b) a C^{1*} element

II. EXTRA DEGREES OF FREEDOM

The addition of extra degrees of freedom to the nodes of an element is one of the most important subjects in finite element method. The extra degrees of freedom were first propounded by Tocher [3] and by Turner and Al [1] in 1965 by presenting a triangular element which was modified later by Clough [4]. This element could not be used in the structures which were subjected to rotational bending. In order to overcome this shortcoming, Tocher and Hartz [1] added the nodal rotations to the triangular nodes and presented an element with 18 degrees of freedom in 1967. This element proved not to be very effective in finite element computations. Further attempts to develop elements capable of handling the corner rotational deformations such as the work by Irons and Ahmad [5] were unsuccessful until 1980's during which Allman [6]

and some other researchers introduced 3-noded triangular elements using quadratic variation for deformation instead of cubic equations as had employed by the previous researchers. One of the most recent attempts has been made by Bigdeli [1] who developed two dimensional elements known as C^* elements. He introduced various order derivatives of the field variable to the nodes and obtained higher convergence and efficiency for their elements. In this work, the work carried out by Bigdeli [1] is extended to three dimensional elements.

III. C^* ELEMENT FAMILY

The first element in the family of two dimensional C^* elements is a 4-noded quadrilateral element shown in Fig. 1(a). The element with only 2 degrees of freedom at each node is called C^{0*} element with the shape functions defined as [2]:

$$N_i = \frac{1}{4}(1 - \xi_i \xi)(1 - \eta_i \eta) \quad (i=1,2,3,4) \quad (4)$$

The second element called C^{1*} and shown in Fig. 1(b) is a 4-noded quadrilateral element with 12 degrees of freedom including the field variable derivatives at each node. This element utilizes the following polynomial for the field variable in each direction [1]:

$$\begin{aligned} \varphi = & a_1 + a_2 \xi + a_3 \eta + a_4 \xi \eta + a_5 \eta^2 + a_6 \xi^2 + a_7 \eta^2 \xi \\ & + a_8 \eta \xi^2 + a_9 \xi^3 + a_{10} \eta^3 + a_{11} \xi^3 \eta + a_{12} \xi \eta^3 \end{aligned} \quad (5)$$

The 12 constants of the equation are obtained using the 12 nodal degrees of freedom in each direction shown in Fig. 1(b). The shape functions of this type of element are given as follows [1]:

$$\begin{aligned} N_1 = & \frac{1}{4} \left[1 - \frac{3}{2} \xi + \frac{1}{2} \xi^3 - \frac{3}{2} \eta + \frac{1}{2} \eta^3 + 2\xi\eta - \frac{1}{2} \xi^3 \eta - \frac{1}{2} \xi \eta^3 \right] \\ N_2 = & \frac{1}{8} \left[1 - \xi - \xi^2 + \xi^3 - \eta + \xi\eta + \xi^2 \eta - \xi^3 \eta \right] \\ N_3 = & \frac{1}{8} \left[1 - \xi - \eta - \eta^2 + \eta^3 + \xi\eta + \xi\eta^2 - \xi\eta^3 \right] \\ N_4 = & \frac{1}{4} \left[1 + \frac{3}{2} \xi - \frac{1}{2} \xi^3 - \frac{3}{2} \eta + \frac{1}{2} \eta^3 - 2\xi\eta + \frac{1}{2} \xi^3 \eta + \frac{1}{2} \xi \eta^3 \right] \\ N_5 = & \frac{1}{8} \left[-1 - \xi + \xi^2 + \xi^3 + \eta + \xi\eta - \xi^2 \eta - \xi^3 \eta \right] \\ N_6 = & \frac{1}{8} \left[1 + \xi - \eta - \eta^2 + \eta^3 - \xi\eta - \xi\eta^2 + \xi\eta^3 \right] \\ N_7 = & \frac{1}{4} \left[1 + \frac{3}{2} \xi - \frac{1}{2} \xi^3 + \frac{3}{2} \eta - \frac{1}{2} \eta^3 + 2\xi\eta - \frac{1}{2} \xi^3 \eta - \frac{1}{2} \xi \eta^3 \right] \\ N_8 = & \frac{1}{8} \left[-1 - \xi + \xi^2 + \xi^3 - \eta - \xi\eta + \xi^2 \eta + \xi^3 \eta \right] \\ N_9 = & \frac{1}{8} \left[-1 - \xi - \eta + \eta^2 + \eta^3 - \xi\eta + \xi\eta^2 + \xi\eta^3 \right] \\ N_{10} = & \frac{1}{4} \left[1 - \frac{3}{2} \xi + \frac{1}{2} \xi^3 + \frac{3}{2} \eta - \frac{1}{2} \eta^3 - 2\xi\eta + \frac{1}{2} \xi^3 \eta + \frac{1}{2} \xi \eta^3 \right] \\ N_{11} = & \frac{1}{8} \left[1 - \xi - \xi^2 + \xi^3 + \eta - \xi\eta - \xi^2 \eta + \xi^3 \eta \right] \\ N_{12} = & \frac{1}{8} \left[-1 + \xi - \eta + \eta^2 + \eta^3 + \xi\eta - \xi\eta^2 - \xi\eta^3 \right] \end{aligned}$$

A C^{1*} quadrilateral element with 12 D.O.F. at each node is depicted in Fig. 2. The field variable function of this element is expressed as follows in each direction:

$$\begin{aligned} \varphi = & a_1 + a_2 \xi + a_3 \eta + a_4 \xi \eta + a_5 \eta^2 + a_6 \xi^2 + a_7 \eta^2 \xi + a_8 \eta \xi^2 \\ & + a_9 \xi^3 + a_{10} \eta^3 + a_{11} \xi^3 \eta + a_{12} \xi \eta^3 + a_{13} \eta^3 \xi^2 + a_{14} \eta^2 \xi^3 \\ & + a_{15} \xi^4 + a_{16} \eta^4 + a_{17} \xi^4 \eta + a_{18} \xi \eta^4 + a_{19} \eta^5 + a_{20} \xi^5 + a_{21} \xi^5 \eta \\ & + a_{22} \eta^5 \xi + a_{23} \xi^3 \eta^3 + a_{24} \xi^2 \eta^2 \end{aligned} \quad (6)$$

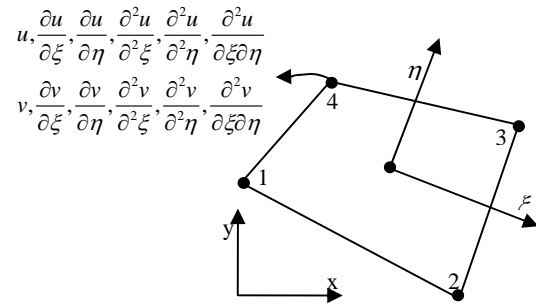


Fig. 2 A C^{1*} element with 12 D.O.F. at each node

IV. 3-D C^{1*} ELEMENT

In the present work we have extended the 2-D dimensional C^* elements to 3-D cases. Since the field variable function of this element and its shape functions are too long, only the 3-D 8-noded C^{1*} element is presented here. This element, as shown in Fig. 3, has 12 D.O.F. at each node.

The field variable function of this element is expressed as follows:

$$\begin{aligned} \varphi = & a_1 + a_2 \xi + a_3 \eta + a_4 \eta^2 + a_5 \xi^2 + a_6 \xi^2 + a_7 \xi \xi \\ & + a_8 \eta \xi + a_9 \xi \eta + a_{10} \eta^3 + a_{11} \xi^3 + a_{12} \xi^3 \\ & + a_{11} \xi^2 \xi + a_{12} \xi \eta^2 + a_{13} \eta \xi^2 + a_{14} \eta^2 \xi + a_{15} \xi^2 \xi \\ & + a_{16} \eta \xi^2 + a_{17} \xi \eta \xi + a_{18} \eta^3 \xi + a_{19} \xi^3 \eta \\ & + a_{20} \xi \eta^3 + a_{21} \eta \xi^3 + a_{22} \xi^3 \xi + a_{23} \xi \xi^3 + a_{22} \eta^2 \xi \xi \\ & + a_{23} \xi^2 \eta \xi + a_{24} \xi \eta \xi^2 + a_{25} \eta \xi^3 \xi + \\ & a_{26} \xi \eta^3 \xi + a_{27} \xi^3 \eta \xi + a_{28} \xi \eta \xi^3 + a_{29} \xi \eta^4 + a_{30} \eta^5 \\ & + a_{31} \xi^5 + a_{32} \xi^5 \eta \end{aligned} \quad (7)$$

The shape functions of this element are lengthy and can be found in reference [7].

V. MAPPING IN 3-D C^{1*} ELEMENTS

In order to achieve mapping for C^* elements we can use their equivalent C^0 elements. For instance, a 32-noded C^0 hexahedron element with 3 D.O.F. at each node can be used for a C^{1*} 8-noded hexahedron element with 12 D.O.F. at each node, as shown in Fig. 4. Therefore, both elements will have 96 D.O.F. The relation between the displacement vectors of the two elements is assumed to be of the form:

$$\{u\} = [T]\{U\} \quad (8)$$

Where $\{u\}$ and $\{U\}$ are the nodal degrees of freedom of C^0 and C^* elements, respectively. The finite element characteristic equation is assumed to be:

$$[k]\{u\} = \{f\} \quad (9)$$

Substituting equation (8) in relation (9) results in the following equation:

$$[k][T]\{U\} = \{f\} \quad (10)$$

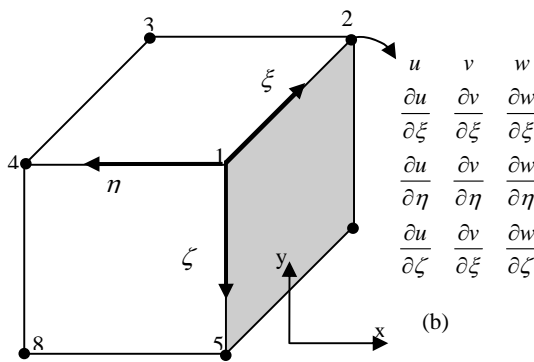
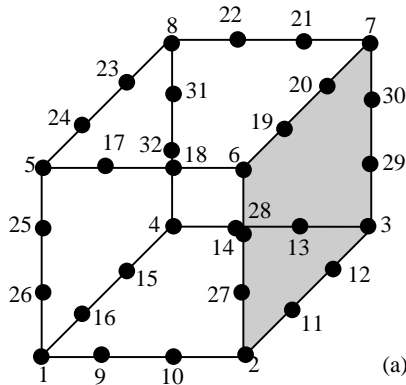


Fig. 4 (a) A 32-noded C^0 element and (b) a hexahedron 8-noded C^* element

If both sides of equation (10) are multiplied by the transpose of the transformation matrix $[T]$, we will obtain:

$$[T]^T [k][T]\{U\} = [T]^T \{f\} \Rightarrow [K]\{U\} = \{F\} \quad (11)$$

$[K]$ and $\{F\}$ are stiffness matrix and force vector of the new element and which are defined as follows:

$$[K] = [T]^T [k][T], \quad \{F\} = [T]^T \{f\} \quad (12)$$

In order to obtain the transformation matrix $[T]$, we can employ the displacement function for the two elements, C^* and C^0 . Let the displacement function for both elements is defined by equation (7). For 32-noded C^0 hexahedron element, this equation can be rewritten as follows:

$$\{u\} = [X]\{a\} \quad (13)$$

Where $\{a\}$ is the vector of the coefficients $a_{i,s}$ in equation (7) and $\{u\}$ is the nodal displacement vector defined as:

$$\{u\} = \{u_1 \ v_1 \ w_1 \ \dots \ \dots\}^T \quad (14)$$

Therefore, the vector of the coefficients $a_{i,s}$ is obtained by solving a linear system of equations with 32 equations. The

matrix form of equation (7) for 8-noded hexahedron C^* element with 12 D.O.F at each node becomes:

$$\{U\} = [B]\{a\} \quad (15)$$

Where $\{U\}$ is the nodal displacement vector defined as:

$$\{U\} = \left\{ U_1 \ v_1 \ w_1 \ \left(\frac{\partial U}{\partial \xi} \right)_1 \ \left(\frac{\partial U}{\partial \eta} \right)_1 \ \left(\frac{\partial U}{\partial \zeta} \right)_1 \ \left(\frac{\partial V}{\partial \xi} \right)_1 \ \left(\frac{\partial V}{\partial \eta} \right)_1 \ \left(\frac{\partial V}{\partial \zeta} \right)_1 \ \left(\frac{\partial W}{\partial \xi} \right)_1 \ \dots \ \dots \right\} \quad (16)$$

Again, the vector of the coefficients $a_{i,s}$ is obtained by solving a linear system of equations with 32 equations:

$$\{a\} = [B]^{-1} \{U\}$$

By substituting this equation in relation (13) we obtain:

$$\{u\} = [X][B]^{-1} \{U\} \quad (17)$$

From the comparison between equations (8) and (17), the transformation matrix, $[T]$, is obtained as follows:

$$[T] = [X][B]^{-1} \quad (18)$$

Once, the transformation matrix is calculated, stiffness matrix, $[K]$, and force vector, $\{F\}$ can be obtained from equation (12).

VI. NUMERICAL RESULTS

The numerical simulation of a cantilever was used to study the performance of C^* elements with the mapping technique used explained in section 3. The cantilever shown in figure 5 is subjected to shear forces applied to the end of the beam as depicted in the figure. An elastic analysis with $E = 200GPa$ and $\nu = 0.3$ was used for the simulation. In order to obtain a better understanding of the performance of C^* elements, the results were compared with those obtained for 8-noded, 20-noded and 32-noded C^0 hexahedron elements. The displacement of the end of the beam and the CPU time were measured from the simulations for each type of element.

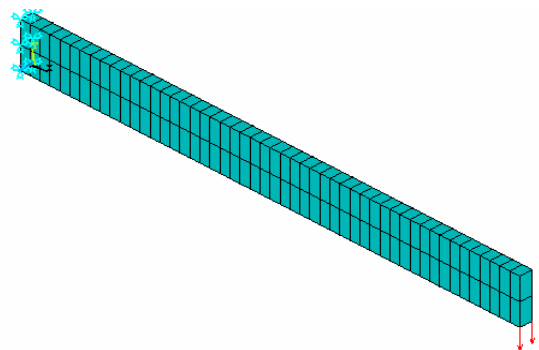


Fig. 5 The finite element model for a beam under bending

The results are illustrated in Figs. 6 and 7 for displacement and CPU time, respectively. As the results shown in Fig. 6 suggest, 8-noded C^* and 32-noded C^0 elements converge more rapidly compared with 20-noded and 8-noded C^0 elements. The convergence rate, however, is nearly the same for 8-noded C^* and 32-noded C^0 elements. The variation of CPU time versus the number of elements is depicted in Fig. 7. The figure clearly shows lower CPU time for 20-noded and 8-noded C^0 elements with respect to 8-

noded C^{1*} and 32-noded C^0 elements. This is obvious as the degrees of freedom of the two latter are less than those of the formers. The interesting point is that the 8-noded C^{1*} element has consumed less CPU time than the 32-noded C^0 . This is while; both elements have the same number of degrees of freedom. Moreover, 8-noded C^{1*} element include first derivatives of displacement components which are physical define the various components of strain. Therefore, the use of 8-noded C^{1*} not only reduces the CPU time with respect to its equivalent C^0 element, but also saves the time for calculation of strains.

3. The convergence rate of 8-noded C^{1*} element is nearly equal to its equivalent C^0 element, while it consumes less CPU time with respect to the C^0 element.
4. The existence of derivative degrees of freedom at the nodes of C^{1*} element along with the privileges mentioned above, makes it superior compared with its equivalent C^0 element.

ACKNOWLEDGMENT

The authors would like to thank Mr B. Bigdeli for his scientific recommendations to this work. Thanks are also due to him for providing us with valuable materials which were very helpful to conduct the present work.

REFERENCES

- [1] B. Bigdeli, An Investigation of C^* Convergence in the Finite Element Method, *Ph.D Thesis*, New South Wales University, Australia, 1996.
- [2] F.L. Stassa, Applied Finite Element Method, CBS International Editions, 1985.
- [3] J.L. Tocher, Analysis of Plate Bending Using Triangular Elements, *Ph.D Dissertation*, University of California, Berkely, 1962.
- [4] R.W. Clough, Comparison of Three Dimensional Finite Elements, *Proceeding of the symposium on Application of Finite Element Method in Civil Engineering*, Vanderbilt University, Nashville, pp. 1-26, 1969.
- [5] S. Ahmad, B.M. Irons, and O.C. Zienkiewicz, Analysis of Thick and Thin Shell Structure by Curved Finite Element, *International Journal for Numerical Methods in Engineering*, 2, 419-451, 1974.
- [6] D.J. Allman, A Compatible Triangular Element Including Vertex Rotation for Plain Elasticity Analysis, *Computers and Structures*, 19, pp. 1-8, 1984.
- [7] B. Sharifi Hamadani, The study of the convergence of C^* elements in 3-D elasticity (in Persian), MSc Thesis, Mechanical Engineering Department, Bu-Ali Sina University, Hammadan, Iran, 2001.

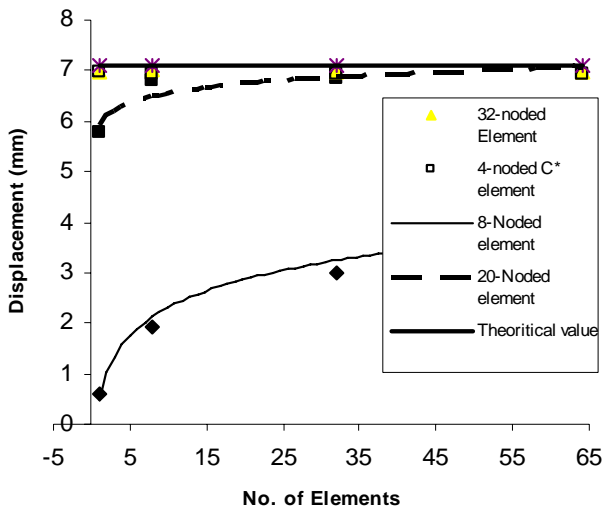


Fig. 6 Variation of displacement versus number of elements for different element types

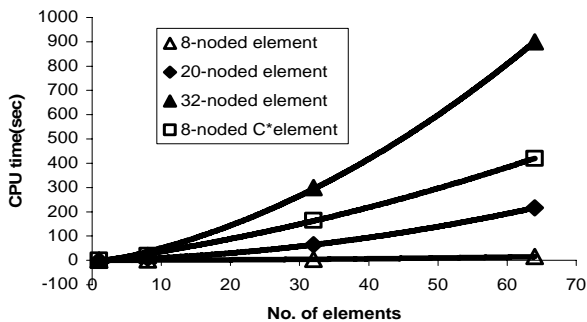


Fig. 7 Variation of CPU-time versus number of elements for different element types

VII. CONCLUSION

From the numerical results, the following conclusions can be derived:

1. Mapping of C^{1*} elements (with extra degrees of freedom) can be forced by a transformation matrix.
2. Transformation matrix can be obtained using equivalent C^0 elements (with the same number of degrees of freedom).